Volume 1 | Number 1 | Jan 2013 | Pages 1–100

ChemComm

Chemical Communications
www.rsc.org/chemcomm

ROYAL SOCIETY OF CHEMISTRY

ROYAL SOCIETY OF CHEMISTRY

www.rsc.org/chemcomm

Composite materials obtained by doping a SBS thermoplastic elastomer matrix with CdSe nanoplatelets show reversible platelets alignment upon stretching.

Journal Name

COMMUNICATION

Strain-controlled fluorescence polarization in a CdSe nanoplatelet / block copolymer composite

E. Beaudoin[a]*, B. Abecassis[a], D. Constantin[a], J. Degrouard[a], P. Davidson[a]

By dispersing semi-conducting CdSe nanoplatelets within a styrene-butadiene-styrene block copolymer matrix we form homogeneous fluorescent hybrid films. Reversible orientation control of the nanoplatelets is simply achieved through stretching the film, leading to tunable fluorescence anisotropy. Such adjustable polarization effects are useful for modulating the optical response in composite materials.

Hybrid materials made of anisotropic metallic or semi-conducting nanoparticles (NPs) dispersed in a polymer matrix have become an exciting class of nanocomposites with promising applications in electronics and optics. For example, the alignment of such materials can improve current transport in electronic devices or modulate the response in optical devices.[1, 2] However, two key points have to be addressed for this purpose. Firstly, a homogeneous dispersion of inorganic nanoparticles in polymeric templates is rather hard to achieve and most often requires surface modification.[3-7] Secondly, the macroscopic orientation of the material, which is required to exploit the anisotropic properties of the individual particles, must be controlled. To date, the orientation of the NPs in polymer matrices is mostly restricted to thin films. For example, nanoparticle alignment could be obtained by stretching a thermoplastic polymer at a temperature close to T_g or by applying an electric field during solvent casting.[2, 8-11] In all cases, the orientation is irreversible, which precludes applications in opto-mechanical devices, for instance. We describe here how we achieved both a homogeneous dispersion of NPs in a thick film and the reversibility of the orientation in a composite material comprised of recently discovered CdSe nanoplatelets (NPLs) dispersed within a classical thermoplastic elastomer matrix. Indeed, CdSe NPLs have attracted much attention due to their outstanding spectroscopic properties.[12-17] These flat and square 2-dimensional photoluminescent nanoparticles display a sharp emission peak that can be precisely tuned by adjusting their thickness at the atomic level. Moreover, they have a very high quantum yield and fast recombination times of the carriers that are confined in one dimension. CdSe NPLs are generally synthesized in solution but they can also be deposited flat on a substrate[18] or aggregated edge-on in micronic needles.[19] The dispersion of nanoparticles in polymers can be improved by using

block copolymers (BCP) as a matrix because the particles are generally confined within one kind of domains.[20, 21] Here, in order to obtain a homogeneous composite material, we carefully adapted the BCP to the oleic acid ligand grafted on the NPLs. The polymer matrix that we have chosen is a thermoplastic elastomer made of Styrene-Butadiene-Styrene (SBS) whose central block is of chemical nature and polarity close to those of oleic acid (Figure 1). A crucial advantage of such a matrix is the possibility to stretch it up to high strain levels in a reversible way at room temperature. We prepared homogeneous CdSe/SBS composite films with a CdSe volume fraction of 10% where both the SBS lamellar microstructure and the CdSe NPL spectroscopic properties are preserved. The CdSe NPLs are square platelets with a homogeneous thickness of 1.2 nm and lateral dimensions of around 10 nm (see ESI for more details on the synthesis and characterization of the CdSe NPLs).
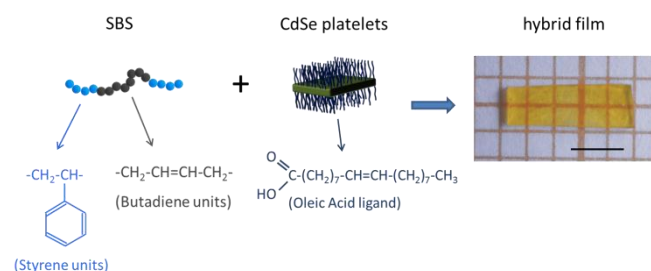

Figure 1. Components of the hybrid film. Left: schematic representation of a SBS copolymer chain. Center: schematic representation of a CdSe nanoplatelet covered with ligands. Right: photography of the hybrid film (Scale bar is 2 mm).

The structural properties of these hybrid films were first studied by Transmission Electron Microscopy (TEM) (Figure 2a). The TEM images, which display light and dark grey bands corresponding to PS and PB domains respectively, clearly confirm the lamellar morphology of the SBS microstructure. Despite the high load in inorganic nanoparticles, the SBS microstructure in the hybrid films

is therefore not much altered compared to that of the pure block copolymer. CdSe platelets have a strong electronic density but are very thin, which explains why the only particles clearly observed on the TEM images are those seen edge-on. Moreover, close inspection of the TEM images reveals that the CdSe platelets are mostly located in the PB domains, which was expected because of the chemical similarity of OA with PB. Very occasionally, a few platelets can be seen in the PS domains, possibly because of some ligand loss during the film preparation (see below). Furthermore, the images show that the platelets self-assemble in short stacks. Indeed, CdSe platelets naturally tend to stack when brought in an unfriendly environment, such as an anti-solvent, in order to maximize ligand-ligand interactions. [19, 22] At this stage, it appears clearly that the growth of the stacks is limited by the rigid PS microdomains.
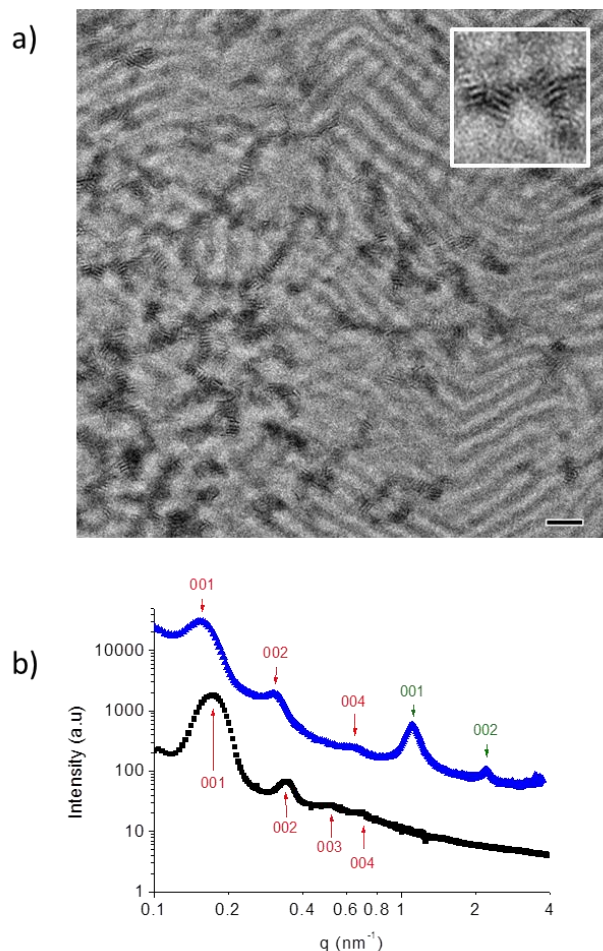

Figure 2. Structure of the hybrid material. a) TEM image of the composite film. Scale bar is 50 nm. Inset is a 3× magnification on NPLs. b) SAXS diagram of a pure SBS film (■) and of the composite film (▲). The reflections arising from the lamellar microstructure of the SBS template are indicated in red whereas the reflections due to the NPL stacking are indicated in green.

The lamellar morphology of the hybrid films is confirmed by their Small-angle X-ray Scattering (SAXS) patterns (Figure 2b) that display diffraction peaks whose positions are in 1:2:3:4 ratios. Moreover, the widths of the (00l) peaks without and with particles remain comparable. However, close inspection of the diffractograms shows that the position of the (001) peak shifts from 0.175 nm^{-1} for pure SBS to 0.155 nm^{-1} for the composite material, which corresponds to an increase in the period of the microstructure from 36 nm without nanoplatelets, to 40 nm in presence of nanoplatelets. This 10% increase in the lamellar period agrees with the volume fraction of CdSe in the film and confirms that the platelets are well dispersed within the microstructure.

Platelet stacking is also detected in reciprocal space at intermediate wave vectors in the SAXS patterns. Two scattering peaks are observed at q = 1.1 nm^{-1} and q = 2.2 nm^{-1}, and correspond to the 001 and 002 reflections of the platelet short stacks. The stacking period of 5.7 nm indicates a 4.5 nm gap between inorganic platelets, in agreement with the presence of almost fully stretched oleic acid molecules on both sides of the NPL. The reflections of both the lamellar microstructure and the platelets stacks are completely isotropic, indicating no preferential orientation in the unstretched films.

Composite films observed by optical fluorescence microscopy display homogeneous fluorescence intensities on the whole field of view, at the micrometer scale, which definitely rules out the presence of macroscopic aggregates (Figure 3a-c). Very importantly, the spectroscopic properties of CdSe nanoplatelets are essentially preserved in the composite films. In all samples, the band-edge exciton emission of the nanoplatelets gives rise to a sharp peak at 519 nm (Figure 3d). This value is slightly but significantly higher than the value of 513 nm recorded for the same platelets dispersed in toluene. It has been previously shown that such energy shifts may arise from changes in the effective size of the nanocrystals due to ligand loss or to ligand exchange reactions.[23] These modifications of the surface of the particles are usually also responsible for deep-trap emission at higher wavelengths (~ 650 nm) because of an increase in surface defects.[23, 24] Therefore, the observation (Figure 3d) of both a redshift of the main peak and a more intense deep-trap emission compared to nanoplatelets in toluene suggests the loss of a small proportion of ligand during the preparation of the films.
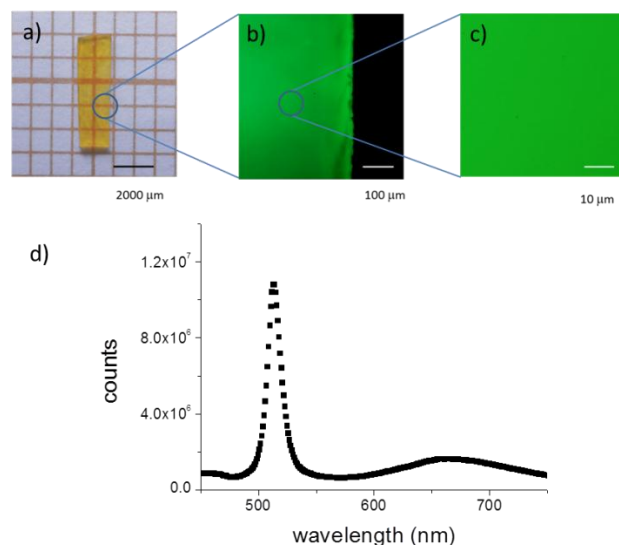

Figure 3. Optical properties of the hybrid material at rest. a) Photograph of the composite film and b) and c) optical fluorescence microscopy images of the same film with FITC filter, at different magnifications. d) Fluorescence spectrum of the same film with excitation at 400 nm.

The CdSe/SBS composite films can easily be stretched up to around 100-150%. The influence of stretching on the structure of the hybrid films was investigated by X-ray scattering (Figure 4). At 100% deformation, almost no scattering signal can be detected when the X-

ray beam is perpendicular to the film. In contrast, very anisotropic signals are observed at both small and intermediate wave vectors when the X-ray beam is parallel to the film. The anisotropy of the SAXS pattern proves that the layers of the block copolymer orient parallel to the film surface. Such orientation is also observed for the pure SBS films. The peak splitting (see Figure 4c) has already been reported in the literature for SBS copolymers and was attributed to a zig-zag texture of the lamellar phase.[25, 26] This texture arises from a mechanical instability upon stretching where lamellar domains alternately reorient at some angle with respect to the stretching direction. X-ray scattering at intermediate q-range (Figure 4d), shows that the platelets align parallel to the lamellar domains (i.e. the platelet normals align parallel to the layer normals). The zig-zag texture also induces a splitting of the stacking reflections of the platelets. The angular spread of the stacking reflections suggests that the platelets are well aligned and it can be used to quantify the orientation degree of the NPLs by calculating the nematic order parameter S.[27] This parameter is 0 for unaligned objects and 1 for perfectly aligned particles. The nematic order parameter S of the platelets reaches here values of the order of S ~ 0.6 at 100% strain, which is quite comparable to the orientational order of usual liquid crystals for instance.
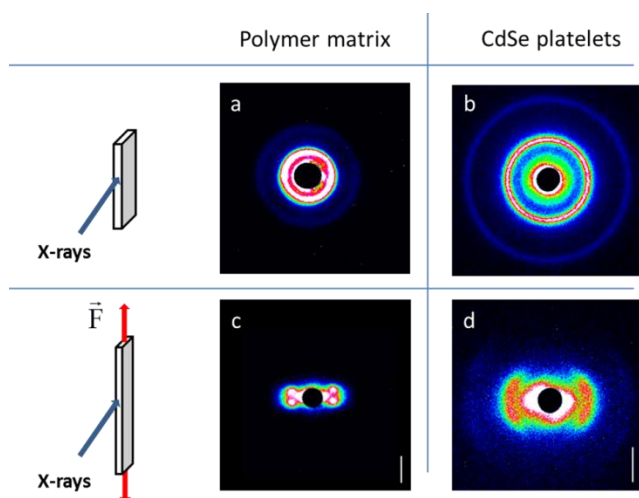

Figure 4. Alignment of the hybrid material by stretching : SAXS patterns of the composite film. a) Scattering from the microdomains of the SBS copolymer at small q-range, without strain. b) Scattering from the stacks of NPLs at intermediate q-range, without strain. c) Scattering from the microdomains of the SBS copolymer at small q-range, 100% strain. d) Scattering from the stacks of NPLs at intermediate q-range, 100% strain. Scale bars on Figures c and d measure 0.2 and 1 nm^{-1}, respectively.

The CdSe NPLs are only weakly confined since their dimensions (~ 10 nm) are smaller than the thickness (~ 20 nm) of the PB domains of the lamellar microstructure. Therefore, the mechanism of orientational coupling of the nanoplatelets with the lamellar matrix may not be purely due to the steric confinement of the NPLs within the lamellar microstructure. Upon stretching, both the layers and the PB chains align parallel to the stretching direction.[26] Then, the CdSe platelets are likely to align parallel to the PB chains in order to avoid altering their conformation.

The photoluminescence of stretched films is highly anisotropic, in contrast with that of unstretched films which is almost isotropic (Figure 5). This can readily be observed visually with a fluorescence microscope equipped with a polarizer. These observations confirm

the fact that the fluorescence light is polarized in the plane of the nanoplatelets.[19] The anisotropy of fluorescence can also be quantified by measuring the photoluminescence intensity with a fluorescence spectrometer using an analyzer placed after the sample. When the analyzer axis is set parallel (resp. perpendicular) to the film, a fluorescence intensity $I_{//}$ (resp. $I_{\perp}$) is measured. The anisotropy is usually quantified by the ratio $r = (I_{\perp} - I_{//})/(2I_{//} + I_{\perp})$.[28] This parameter r increases from 0 for the film at rest to ~ - 0.25 for the film at 100% strain. A simple model (see ESI) gives $r = - S/2$, so that S ~ 0.50, in fair agreement with the value (S ~ 0.60) previously obtained by X-ray scattering. This confirms that film stretching gives rise to a strong orientation of the nanoplatelets and a highly anisotropic photoluminescence, with light emission polarized parallel to the film. The level of anisotropy depends on the strain and the samples become again isotropic when the stress is removed and deformation relaxes (see supplementary information for some cycles of stretching and relaxation).
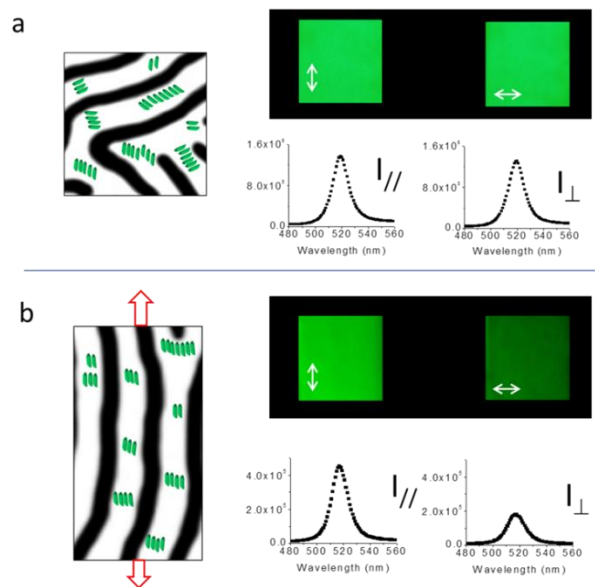

Figure 5. Effect of stretching on the fluorescence properties of the hybrid material: schematic representation of a composite film, optical microscopy and emission spectra of, a) film at rest showing isotropic photoluminescence; b) stretched film (100% strain) showing anisotropic photoluminescence. The white arrows represent the direction of the analyzer.

Conclusions

Homogeneous dispersion of semiconducting nanoplatelets in a thick film was achieved by carefully selecting a thermoplastic BCP matrix compatible with the ligand brush grafted on the nanoparticles. Moreover, the tendency of CdSe NPLs to stacking is limited by the confinement within the PB domains of the BCP structure at the microscopic scale, resulting in optically homogeneous composite materials. Stretching these composites provides an easy way of controlling particle orientation. This alignment is reversible as relaxing the samples immediately restores the initial isotropic distribution of the nanoplatelets. From a fundamental point of view, this allows investigating in detail the NPL anisotropic physical properties,

as was shown above in the case of photoluminescence. From a more applied point of view, polarization effects are useful for modulating the optical response (absorption and/or photoemission) in materials. For example, the polarized photoemission of aligned CdSe NPLs could prove useful for emitters in lasers,[29] because the concentration of the emission in a single polarization state may reduce the operating power. More generally, the present approach may be also applied to other types of composite films comprised of nanosheets, such as graphene or clays, whose mechanical or barrier properties strongly depend on filler orientation.

Notes and references

[a] Laboratoire de Physique des Solides, Université Paris-Sud, CNRS, UMR 8502, 91405 Orsay, France

*Corresponding author's contact email: emmanuel.beaudoin@u-psud.fr

1. W. U. Huynh, J. J. Dittmer and A. P. Alivisatos, *Science*, 2002, **295**, 2425-2427.
2. J. Perez-Juste, B. Rodriguez-Gonzalez, P. Mulvaney and L. M. Liz-Marzan, *Adv Funct Mater*, 2005, **15**, 1065-1071.
3. A. C. Balazs, T. Emrick and T. P. Russell, *Science*, 2006, **314**, 1107-1110.
4. Q. Lan, L. F. Francis and F. S. Bates, *J Polym Sci Pol Phys*, 2007, **45**, 2284-2299.
5. E. Glogowski, R. Tangirala, T. P. Russell and T. Emrick, *J Polym Sci Pol Chem*, 2006, **44**, 5076-5086.
6. J. Lee, V. C. Sundar, J. R. Heine, M. G. Bawendi and K. F. Jensen, *Adv Mater*, 2000, **12**, 1102-+.
7. S. Fischer, A. Salcher, A. Kornowski, H. Weller and S. Forster, *Angew Chem Int Edit*, 2011, **50**, 7811-7814.
8. B. M. I. van der Zande, L. Pages, R. A. M. Hikmet and A. van Blaaderen, *J Phys Chem B*, 1999, **103**, 5761-5767.
9. S. Gupta, Q. L. Zhang, T. Emrick and T. P. Russell, *Nano Lett*, 2006, **6**, 2066-2069.
10. M. J. A. Hore and R. J. Composto, *Macromolecules*, 2014, **47**, 875-887.
11. R. A. M. Hikmet, P. T. K. Chin, D. V. Talapin and H. Weller, *Adv Mater*, 2005, **17**, 1436-+.
12. S. Ithurria, M. D. Tessier, B. Mahler, R. P. S. M. Lobo, B. Dubertret and A. Efros, *Nat Mater*, 2011, **10**, 936-941.
13. S. Ithurria and B. Dubertret, *J Am Chem Soc*, 2008, **130**, 16504-+.
14. K. P. Rice, A. E. Saunders and M. P. Stoykovich, *J Am Chem Soc*, 2013, **135**, 6669-6676.
15. M. Pelton, S. Ithurria, R. D. Schaller, D. S. Dolzhnikov and D. V. Talapin, *Nano Lett*, 2012, **12**, 6158-6163.
16. A. W. Achtstein, A. Schliwa, A. Prudnikau, M. Hardzei, M. V. Artemyev, C. Thomsen and U. Woggon, *Nano Lett*, 2012, **12**, 3151-3157.
17. Y. Kim, N. W. Song, H. Yu, D. W. Moon, S. J. Lim, W. Kim, H. J. Yoon and S. K. Shin, *Phys Chem Chem Phys*, 2009, **11**, 3497-3502.
18. D. S. Chung, J. S. Lee, J. Huang, A. Nag, S. Ithurria and D. V. Talapin, *Nano Lett*, 2012, **12**, 1813-1820.
19. B. Abecassis, M. D. Tessier, P. Davidson and B. Dubertret, *Nano Lett*, 2014, **14**, 710-715.
20. A. Haryono and W. H. Binder, *Small*, 2006, **2**, 600-611.
21. R. A. Vaia and J. F. Maguire, *Chem Mater*, 2007, **19**, 2736-2751.
22. M. D. Tessier, L. Biadala, C. Bouet, S. Ithurria, B. Abecassis and B. Dubertret, *Acs Nano*, 2013, **7**, 3332-3340.
23. G. Kalyuzhny and R. W. Murray, *J Phys Chem B*, 2005, **109**, 7012-7021.
24. S. R. Cordero, P. J. Carson, R. A. Estabrook, G. F. Strouse and S. K. Buratto, *J Phys Chem B*, 2000, **104**, 12137-12142.
25. T. Hashimoto, M. Fugimura, K. Saijo, H. Kawai, J. Diamant and M. Shen, *Adv. Chem. Ser.*, 1979, **176**, 257-275.
26. T. A. Huy, R. Adhikari and G. H. Michler, *Polymer*, 2003, **44**, 1247-1257.
27. E. Paineau, I. Dozov, A. M. Philippe, I. Bihannic, F. Meneau, C. Baravian, L. J. Michot and P. Davidson, *J Phys Chem B*, 2012, **116**, 13516-13524.
28. J. R. Lakowicz, *Principles of fluorescence spectroscopy*, Springer, Baltimore, USA, 2006.
29. C. She, I. Fedin, D. S. Dolzhnikov, A. Demortiere, R. D. Schaller, M. Pelton and D. V. Talapin, *Nano Lett*, 2014, **14**, 2772-2777.